JPET Fast Forward. Published on March 3, 2016 as DOI: 10.1124/jpet.115.231100
This article has not been copyedited and formatted. The final version may differ from this version.

JPET #231100

Rescue of Synaptic Phenotypes and Spatial Memory in Young Fragile X Mice

Miao-Kun Sun, Jarin Hongpaisan, and Daniel L. Alkon

Blanchette Rockefeller Neurosciences Institute, 8 Medical Center Drive

Morgantown, WV 26505

JPET Fast Forward. Published on March 3, 2016 as DOI: 10.1124/jpet.115.231100
This article has not been copyedited and formatted. The final version may differ from this version.

Running title: Rescuing synapses and spatial memory in young fragile X mice

Correspondence and requests for materials should be addressed to:

Miao-Kun Sun, Blanchette Rockefeller Neuroscience Institute, 8 Medical Center Dr., Morgantown, WV 26505, USA; Phone: 304-293-1701; Fax: 304-293-7536; E-mail: masun@brni.org and mksun@brni-jhu.org.

The number of text pages: 36

tables: 0

figures: 5

references: 56

The number of words in the Abstract: 236

Introduction: 509

Discussion: 1,507

A recommended section: Behavioral Pharmacology

Abbreviations

BDNF, brain-derived neurotrophic factor

DiL, 1,1'-Dioctadecyl-3,3,3',3'-Tetramethylindocarbocyanine Perchlorate

FMR1, fragile X mental retardation 1

FMRP, fragile X mental retardation protein

FXS, fragile X syndrome

GAP, growth-associated protein

GSK3β, glycogen synthase kinase 3β

mGluR, metabotropic glutamate receptor

PBS, phosphate buffered saline

PKC, protein kinase C

PSD, postsynaptic density

PSF, point spread function

JPET Fast Forward. Published on March 3, 2016 as DOI: 10.1124/jpet.115.231100
This article has not been copyedited and formatted. The final version may differ from this version.

Abstract

Fragile X syndrome (FXS) is characterized by synaptic immaturity, cognitive impairment, and behavioral changes. The disorder is caused by transcriptional shutdown in neurons of the *FMR1* gene product, fragile X mental retardation protein (FMRP). FMRP is a repressor of dendritic mRNA translation and its silencing leads to dysregulation of synaptically driven protein synthesis and impairments of intellect, cognition, and behavior, a disorder which currently has no effective therapeutics. Here, young fragile X mice were treated with chronic bryostatin-1, a relatively selective PKCε activator, which induces synaptogenesis and synaptic maturation/repair. Chronic treatment with bryostatin-1 rescues young fragile X mice from the disorder phenotypes, including normalization of most FXS abnormalities in 1) hippocampal brain-derived neurotrophic factor (BDNF) expression, 2) the PSD-95 levels, 3) transformation of immature dendritic spines to mature synapses, 4) densities of the presynaptic and postsynaptic membranes, and 5) spatial learning and memory. The therapeutic effects were achieved without down-regulation of mGluR5 in the hippocampus and are more dramatic than those of a late-onset treatment in adult fragile X mice. The mGluR5 expression was in fact lower in fragile X mice and its expression was restored with the bryostatin-1 treatment. Our results show that synaptic and cognitive function of young FXS mice can be normalized through pharmacological treatment without down-regulation of mGluR5 and that bryostatin-1-like agents may represent a novel class of drugs to treat fragile X mental retardation at a young age and in adults.

JPET Fast Forward. Published on March 3, 2016 as DOI: 10.1124/jpet.115.231100
This article has not been copyedited and formatted. The final version may differ from this version.

Introduction

Fragile X syndrome (FXS), the most common form of inherited intellectual disability (Santoro et al., 2012), is characterized by synaptic immaturity, cognitive deficits (Koekkoek et al., 2005), and autistic-like behavior (Sabaratnam et al., 2003). The disorder is typically caused by an expansion of an untranslated CGG repeat in the 5' untranslated region of the X-linked gene *fragile X mental retardation 1* (*FMR1;* Verkerk et al., 1991). This triplet expansion leads to DNA methylation of *FMR1* and transcriptional shutdown of the gene. The loss of the fragile X mental retardation protein (FMRP), an RNA-binding protein, causes dysregulation of the translation of dendritic mRNAs (Ashley *et al*., 1993; Darnell and Klann, 2013). FMRP represses translation probably by interacting with a specific subset of mRNAs, directly binding to the ribosome with high affinity, and thereby precluding the binding of tRNA and translation elongation factors on the ribosome (Chen et al., 2014). The key functional role of the binding of FMRP to RNA is supported by the evidence that a missense mutation in the KH2 domain (Ile304Asn) of human FMRP abolishes its binding to polyribosome and leads to a severe form of FXS (Siomi *et al*., 1994).

Signal processing at synapses is dramatically altered due to the lack of FMRP, resulting in an impaired ability in synaptogenesis, synaptic maturation, and synaptic plasticity to meet cognitive demands (Nelson and Alkon, 2015) and behavioral control. The most compelling is the evidence involving the metabotropic glutamate receptor 5 (mGluR5; Bhattacharya and Klann, 2012), based on the observation of an abnormally enhanced mGluR5-dependent long-term depression in fragile X mice (Huber et al., 2002). The leading 'mGluR theory of FXS indicates that overactive mGluR5 signaling, normally balanced by FMRP, underlies much of the brain pathology of FXS (Santoro et al., 2012; Hajós, 2014). Drug development for the treatment of FXS thus has been

focused on achieving this balance by reducing the mGluR5 hyperactivity in the brain. Consistently, genetic reduction of mGluR5 expression or pharmacologic mGluR5 antagonism has been reported to correct many FXS phenotypes in fragile X mice (Huber et al., 2002; Hajós, 2014).

We have found that chronic activation of PKCε in the hippocampus can rescue synapses and spatial cognition, as well as other FXS phenotypes, in adult fragile X mice after the disorder has established (Sun et al., 2014). The downside of the late-onset treatment is that the therapy may miss a critical period of youth, important in age-related socio-cognitive and behavioral development. It is also not clear whether the observed therapeutic effects involve down-regulation of the mGluR5 in the hippocampus. If the syndrome is a lasting consequence of brain development with deficit in synaptic maturation, it is possible that early intervention with agents that facilitate synaptic maturation could achieve a better outcome, unfolding full potential of therapeutics. This is highly achievable, considering the evidence that newborn screening for FXS is technically feasible (Tassone, 2014). In this study, we, therefore, evaluate therapeutic potential of a PKCε activator on synapses, cognitive function, and other FXS phenotypes, including mGluR5 expression in the hippocampus of young fragile X mice.

JPET Fast Forward. Published on March 3, 2016 as DOI: 10.1124/jpet.115.231100
This article has not been copyedited and formatted. The final version may differ from this version.

Materials and Methods

Animals and drug treatment

Two types of mice (male, The Jackson Laboratories, ME, USA; 9-10/group; at an age of close to 3 weeks when obtained) were used: FVB.129P2-*Pde6b*$^{+}$ *Tyr*$^{c\text{-}ch}$ *Fmr1*^{tm1Cgr}/J (fragile X mice) and FVB.129P2-*Pde6b*$^{+}$ *Tyr*$^{c\text{-}ch}$/AntJ (age-matched wild-type controls). These mice do not suffer from blindness. They were housed in a temperature-controlled (20-24°C) room, allowed free access to food and water, and kept on a 12-hour light/dark cycle.

All mice were randomly assigned to different groups. Bryostatin-1 was administered (20 μg/m^2, tail i.v., 2 doses/week for 6 weeks), starting at an age of close to 4 weeks (26-27 days). The treatment would catch the last week or so in brain development (A month in a mouse with a lifespan of 2 years is roughly equal to 3.3 years of brain development in humans; Sengupta, 2013) before FXS phenotypes are established in the fragile X mice (Bhattacharya and Klann, 2012). Although synaptogenesis and synaptic maturation occur throughout a mammalian lifespan, the mouse brain development is anatomically complete at about 5 weeks of age, when all FXS phenotypes are established in the fragile X mice (Michalon et al., 2012; Bhattacharya and Klann, 2012). The age would roughly correspond to mid-adolescence (~15 years of age) in human in term of synaptic maturation in the prefrontal cortex (Huttenlocher and Dabholkar, 1997). The same behavioral training procedures were performed in all animal groups in the study, so that differences in observed results would indeed reflect impacts of drug treatments. The dose was based on our preliminary dose-response studies that smaller doses were not effective against disorders-induced synaptic and cognitive impairments. Non-treated groups received the same volume of vehicle at the same frequency. Synaptic and memory functions and other phenotypic features were evaluated 9 days after the last dose.

JPET Fast Forward. Published on March 3, 2016 as DOI: 10.1124/jpet.115.231100
This article has not been copyedited and formatted. The final version may differ from this version.

Tissue preparation for confocal microscopy

Animals were deeply anesthetized with sodium pentobarbital (120 mg/kg, i.p.) and perfused through the heart with phosphate buffered saline (PBS) for <4 min at room temperature and then with 4% paraformaldehyde in PBS (≈ 40 ml) to remove any negative impact of hypothermia on dendritic spines (Kirov et al., 2004). Brains were then kept in 4% paraformaldehyde in PBS for 10 min at 4°C and stored in PBS at 4°C. Right dorsal hippocampi were sectioned with a vibratome (Leica VT1200S) into 200 μm thickness and kept in series in PBC at 4°C for 3-D reconstruction.

3D reconstruction analysis of dendritic spine morphology on dendritic shafts

The tips of glass electrodes, prepared for electrophysiological experiments, were immersed for 10s in 5% (w/v) 1,1'-Dioctadecyl-3,3,3',3'-Tetramethylindocarbocyanine Perchlorate (DiI) in dichloromethane (Sigma-Aldrich) and air-dried at room temperature for 1 hour (twice). The tips of DiI-coated electrodes were inserted, broken, and left in the strata oriens of CA1 area of hippocampal sections at 200 μm thickness (3-4 electrode tips/slice). After maintenance in PBS at 4°C overnight, the hippocampal sections were resectioned to 7 μm thickness and kept in PBS at 4°C. In case that DiI was not well diffused along dendritic shafts, the 7-μm thickness sections in PBS were changed from 4°C to room temperature. At each time of confocal scanning, only one section was freshly mounted on a silane-coated microscope slide (SilanatedTM Slides, KD Medical, Columbia, MD), using 4% paraformaldehyde in PBS as a mounting medium.

Dendrites were imaged by a Zeiss Axio Observer Z1 microscope equipped with a 710-confocal scanning microscopy (>510 nm/568 nm; excitation/emission) using 100x Plan-APO

JPET Fast Forward. Published on March 3, 2016 as DOI: 10.1124/jpet.115.231100
This article has not been copyedited and formatted. The final version may differ from this version.

Chromat oil immersion objective (1.4 NA). A series of randomized confocal images (1024x1024 pixels) were confocally scanned at every 0.145 μm. The image resolution was according to Nyquist sampling, a pixel size was 48, 48, and 145 (x, y, and z in nm). Using the ImageJ plugin Deconvolution Lab (Biomedical Imaging Group, EPFL; Lausanne, Switzerland), stacks of confocal images were deconvoluted by the Tikhonov-Miller algorithm. A confocal stack of point spread function (PSF), used for deconvolution, was prepared from Fluoro-max dyed red aqueous fluorescent beads (63 nm diameter, 1% w/v stock solution; Thermo Fisher Scientific, Fremont, CA); further diluted to 1:10,000, smeared, and air-dried on a microscopic slide coated with 0.01% poly-L-lysine.

Dendritic spines were automatically detected and counted with NeuronStudio (beta) program (Rodriguez *et al.*, 2008; http://research.mssm.edu/cnic/tools-ns.html). Dendritic projections from dendritic shafts at 0.2-3 μm length were classified as dendritic spines. Dendritic spines with head to neck diameter ratio (Neck Ratio) greater than 1.1 were either considered as thin or mushroom spines (see below). Spines that were not met the Neck Ratio value (head to neck diameter ratio of greater than 1.1) and had a length of spine to head diameter (Thin Ratio) above 2.5 were automatically classified as thin, otherwise as stubby. Spines that met the Neck Ratio value and had a head diameter (Mushroom Size) equal or greater than 600 nm (Sorra and Harris, 2000) were automatically labeled as mushroom, otherwise as stubby. Filopodia were identified manually (long profiles without enlarged heads) from the projection structures that was longer than dendritic spines and did not have enlarged heads.

Immunohistochemistry

While histochemical levels of PSD-95 or synaptophysin have been found to correspond well

with those detected at the biochemical levels (Glantz et al., 2007; Horling et al., 2015), Western blots measure the total protein levels in the tissue and may have results different from histochemistry at a single structure or cell level, due to protein expression or transport to specific structure (Hongpaisan et al. (2013). The present study, however, focused on the structure changes and we therefore used immunohistochemistry to confirm the morphological studies: EM (see below) and confocal microscopy of DiI staining.

Hippocampal sections at 200 μm thickness were further fixed in 4% paraformaldehyde in PBS for 2-3 days at 4°C and resectioned into 5 μm thickness. Sections at 5 μm thickness of the right dorsal hippocampus (1 section every 400 μm; 4 serial sections from each animal) were processed as described below. Hippocampal slices were incubated free-floating with Image-iTTM FX signal enhancer (Thermo Fisher Scientific/Life Technologies, Grand Island, NY) for 30 min at room temperature. Sections were incubated overnight at room temperature with primary antibodies (Hongpaisan and Alkon, 2007): mouse monoclonal anti-synaptophysin (1:2,000; EMD Millipore, Billerica, MA); rabbit polyclonal anti-spinophilin (1:100; EMD Millipore); mouse monoclonal anti-growth-associated protein (GAP)-43/B-50 (1:2,000; EMD Millipore); mouse monoclonal anti-postsynaptic density (PSD)-95 (1:100; Santa Cruz Biotechnology, Santa Cruz, CA); mouse monoclonal anti-BDNF (1:50; Santa Cruz Biotechnology); and/or rabbit monoclonal anti-mGluR5 (1:100; Abcam, Cambridge, MA). Tissue sections were then incubated with either Alexa Fluor 568 secondary antibody (1:200; Thermo Fisher Scientific) and/or a biotinylated secondary antibody (1:20; Vector Laboratories, Burlingame, CA) for 3 hours at room temperature and then streptavidin-conjugated Alexa Fluor 488 (1:100; Thermo Fisher Scientific) for 3 hours at room temperature. Sections were mounted with VECTASHIELD mounting medium with DAPI to counterstain nuclei (Vector

JPET Fast Forward. Published on March 3, 2016 as DOI: 10.1124/jpet.115.231100
This article has not been copyedited and formatted. The final version may differ from this version.

Laboratories).

The random area in hippocampal CA1 stratum radiatum that appeared immediately after switching to higher magnification lens, 63X Plan-APO Chromat oil immersion objectives (1.4 NA), was imaged for appropriate fluorescence (e.g., Alexa 488 and/or 568). Confocal images of hippocampal sections were acquired in line-scan mode and with a pinhole of approximately 1.00 Airy unit. Confocal images with similar levels of DAPI fluorescence intensity among experimental conditions were quantified with the ImageJ program (http://rsb.info.nih.gov/ij/), with control data being set at 100%.

Quantification for immunostained density of pre- or postsynaptic structure

Confocal images of the density of postsynaptic dendritic spines, presynaptic axonal terminals, postsynaptic membranes, or presynaptic membranes per 45 x 45 x 0.6 μm^3 volume of the CA1 stratum radiatum were analyzed as previously described (Hongpaisan et al., 2011).

Electron microscopy

Under anesthesia with pentobarbiturate, mice were perfused through the heart with PBS (5 ml) and 2% glutaraldehyde and 3% paraformaldehyde in PBS (80 ml). Brains were removed and stored in fixative at 4°C. Hippocampal slices were processed for Epon-embedding, resectioned to 90 nm thickness, collected on a grid, and stained with uranyl acetate and lead citrate. Electron micrographs were taken of the middle of each section with a JEOL 1010 transmission electron microscope. Random sampling was achieved by orienting the hippocampal CA1 area under low-power magnification. The random area that immediately appeared after switching to a higher magnification (7,000X magnification) was imaged with a CCD camera. Electron micrographs

JPET Fast Forward. Published on March 3, 2016 as DOI: 10.1124/jpet.115.231100
This article has not been copyedited and formatted. The final version may differ from this version.

were quantified on the program Preview on a MacPro 4.1 computer with a 30-inch monitor (Apple, Cupertino, CA). Electron micrographs were collected within a 14x14x0.09 μm^3 of the CA1 stratum radiatum. We defined axospinous synapses as those located between dendritic spine structures that do not contain mitochondria and with axon boutons containing presynaptic vesicles.

Spatial learning and memory and visible platform test

A modified Morris water-maze task (2 trials/day for 8 days), a difficult task for revealing mild impairments, was used to evaluate spatial learning and memory.

Water maze training sessions began on the 9th day after the last dose of bryostatin-1, a time gap to separate potential acute effects from the chronic therapeutic impacts. The maze pool had a diameter of 114 cm and height of 60 cm and was filled with 40 cm H_2O (22±1°C), mixed with 200 ml of non-toxic white Tempera (BesTemp, Certified Color Corp, CA). Mice were trained to find a hidden platform, centered in one of the quadrants and submerged 2 cm below the water surface. At the start of each trial, mice were placed individually in the water facing the maze wall, using different starting positions each trial, and allowed to swim until they find the platform, where they remained for 20 s. If a mouse failed to find the platform within 1.5 min, it would be guided there by the investigator, with 90 s scored. The swim path was recorded with a video-tracking system. After the training trials, a probe trial was given, 24 hours after the last training trial, with the platform removed to assess memory retention for its location by the distance the mouse moved in the quadrants. The video-tracking system tracked the animal's movements in each quadrant (1 minute).

The sensorimotor ability of mice was evaluated with a visible platform test. The platform was placed at a new location and was marked with a pole that protruded 9 inches above the water surface.

Statistical analysis was performed using the analysis of variance (ANOVA), followed by Newman-Keuls multiple comparisons test. $P<0.05$ was considered statistically significant. All procedures were conducted according to National Institutes of Health Animal Care and Use Committee guidelines and approved by the Ethical Committee of the Institute.

JPET Fast Forward. Published on March 3, 2016 as DOI: 10.1124/jpet.115.231100
This article has not been copyedited and formatted. The final version may differ from this version.

Results

Bryostatin-1 Improves the Levels of PSD-95 and Metabotropic Glutamate Receptors in young fragile X mice

Significant differences among experiment groups for postsynaptic density protein 95 (PSD) membranes, primarily accumulated in the postsynaptic membranes ($F_{3,222}$=6.121, P<0.001; Figure 1A,B) were observed. In wild-type mice, bryostain-1 significantly increased postsynaptic membranes (P<0.01; Figure 1B). Fragile X mice showed significant decreases in the densities of postsynaptic membranes (P<0.05; Figure 1B). Bryostatin-1 improved the formation of postsynaptic membranes (P<0.001; Figure 1B) in fragile X mice. The data using immunohistochemistry confirmed the results from electron microscopy (see below).

Accumulation of mGluR5 into postsynaptic densities was examined with the colocalization of mGluR5 and PSD-95, using immunohistochemistry and confocal microscopy (Figure 1A). Significant differences among wild-type mice (WC), wild-type mice with bryostatin-1 (WB), fragile X mice (TC), and fragile X mice with bryostatin-1 (TB) groups were observed for the density of mGluR5-containing postsynaptic membranes (colocalization area of mGluR5 and PSD-95; ANOVA, $F_{1,187}$=7.814, P<0.001; Figure 1C) and mGluR5 level in postsynaptic membranes (mGluR5 fluorescence intensity in the colocalization area; $F_{1,187}$=3.478, P<0.01; Figure 1D). Data with significant difference with ANOVA were subsequently analyzed with two-tailed paired T-test. Bryostatin-1 had no effect in wild-type mice, whereas in transgenic mice, decreases in the number of mGluR5-containing postsynaptic membranes (P<0.01; Figure 1C) and their mGluR5 level (P<0.05; Figure 1D) were significantly improved with bryostatin-1 (P<0.01; Figure 1C,D). Bryostatin-1 also enhanced the density of mGluR5-containing

JPET Fast Forward. Published on March 3, 2016 as DOI: 10.1124/jpet.115.231100
This article has not been copyedited and formatted. The final version may differ from this version.

postsynaptic membranes in transgenic mice, compared to wild-type controls (Figure 1C, compared TB with WC).

Bryostatin-1 prevents the Loss of Brain-Derived Neurotrophic Factor in young fragile X mice

Immunohistochemistry of BDNF in the CA1 stratum radiatum, imaged with a confocal microscope, showed a significant difference among experimental groups ($F_{1,120}$=27.484, P<0.001; Figure 1E). Bryostatin-1 did not increase BDNF expression in wild-type mice (Figure 1F). However, Figure 1E showed that in transgenic mice, the reduction of BDNF (P<0.001) was significantly improved (P<0.001) and even elevated above wildtype levels (compared TB with WC; P<0.05) with bryostatin-1.

Bryostatin-1 Increases Presynaptic Vesicle Concentration within Presynaptic Boutons

Densities of presynaptic axonal boutons and their presynaptic vesicle content in the hippocampal CA1 stratum radiatum were evaluated with confocal immunohistochemistry (Figure 2A). ANOVA showed no significant difference among experimental groups for presynaptic axonal bouton density, as determined by counting the grains of presynaptic vesicle protein synaptophysin (Figure 2B). However, significant differences among experiment groups were seen for presynaptic vesicle concentration within the presynaptic axonal boutons, as determined with the fluorescent intensity of synaptophysin ($F_{3,142}$=2.726, P<0.05; Figure 2C). Although bryostatin-1 had no effect on presynaptic bouton density in all experimental conditions (Figure 2B), bryostatin-1 increased presynaptic vesicle concentration within the presynaptic boutons both in wild-type (P<0.05) and fragile X (P<0.01) mice (Figure 2C).

JPET Fast Forward. Published on March 3, 2016 as DOI: 10.1124/jpet.115.231100
This article has not been copyedited and formatted. The final version may differ from this version.

Electron microscopy was further used to determine the concentration of presynaptic vesicles at a single axonal bouton level (Figure 2E). There was a significant difference among experimental groups ($F_{3,190}$=8.018, P<0.001; Figure 2D). Electron microscopy confirmed the results of confocal immunohistochemistry that no significant change in presynaptic vesicles level was observed in the fragile X mice (Figure 2D, compared TC with WC), and bryostyatin-1 significantly increased presynaptic vesicle level in both wild-type and fragile X mice (Figure 2D, WB vs. WC, and TB vs. TC).

Bryostatin-1 Increases Synaptic Densities

Density of axodendritic synapses in the hippocampal CA1 stratum radiatum was determined with electron microscopy (Figure 3A). There was a significant difference among experimental groups ($F_{3,195}$=6.426, P<0.001; Figure 3B). In wild-type mice, bryostatin-1 significantly increased synaptic density (P<0.05; Figure 3B). In fragile X mice, synaptic loss (P<0.05) was significantly reversed (P<0.001) with bryostatin-1 treatment (Figure 3B).

Changes in presynaptic membranes in the hippocampal CA1 stratum radiatum were further studied, using confocal immunohistochemistry (Figure 3C). Significant differences among experiment groups for growth-associated protein 43 (GAP-43), predominantly located in presynaptic membranes ($F_{3, 117}$=13.149, P<0.001; Figure 3D), were observed. In wild-type mice, bryostain-1 significantly increased presynaptic membranes (P<0.05; Figure 3D). Fragile X mice showed significant decreases in the densities of presynaptic membranes (P<0.001; Figure 3D). Bryostatin-1 improved the formation of presynaptic membranes (P<0.05; Figure 3D). The data using immunohistochemistry confirmed the results from electron microscopy (see below).

JPET Fast Forward. Published on March 3, 2016 as DOI: 10.1124/jpet.115.231100
This article has not been copyedited and formatted. The final version may differ from this version.

In the wild-type mice, bryostatin-1 increased the synaptic density (Figure 3A-E), but not the dendritic spine density (Figure 3I,K), suggesting that some dendritic spines form more than one synapse.

Bryostatin-1 Increases Mushroom-Shape Dendritic Spine Formation

Change of the dendritic spine number at a single apical dendrite level in the hippocampal CA1 pyramidal neuron was studied with DiI staining and imaged with a confocal microscopy (Figure 3E). A significant difference among experimental groups for mushroom dendritic spines was seen ($F_{3,142}$=7.186, P<0.001; Figure 3F).

In wild-type mice, bryostatin-1 significantly elevated the number of mushroom spines per 100 μm dendritic shaft above wild-type levels (P<0.05; Figure 3F, compared WB with WC), correlated with the enhancement of memory retention after water maze training. In the fragile X mice, a significant decrease in mushroom dendritic spines (P<0.01; Figure 3F, compared TC with WC) was significantly improved with bryostatin-1 treatment (P<0.001; Figure 3F, compared TB with TC). The number of mushroom spines in fragile X mice treated with bryostatin-1 was not different from that in wild-type mice treated with bryostatin-1 (Figure 3F, compared TB with WB).

Bryostatin-1 Improves the Maturation of Dendritic Spines in young fragile X Mice

Significance differences among experimental groups were found for immature spines or filopodia ($F_{3,142}$=24.386, P<0.001; Figure 3G) and mature dendritic spines (mushroom+thin+stubby spines; $F_{3,142}$=3.956, P<0.01; Figure 3H) were seen at a single apical dendritic shaft of the CA1 pyramidal neuron. In wild-type mice, bryostatin-1 treatment did not

JPET Fast Forward. Published on March 3, 2016 as DOI: 10.1124/jpet.115.231100
This article has not been copyedited and formatted. The final version may differ from this version.

change the numbers of filopodia and mature dendritic spines (Figure 3G,H). In the fragile X mice, an increased number of immature spines ($P<0.001$; Figure 2H) and a decreased number of mushroom+thin+stubby spines ($P<0.05$; Figure 3H) were observed compared to wild-type mice. These changes were reversed to the wild-type control level with bryostatin-1 treatment.

Changes in overall dendritic spine density (45 x 45 x 0.6 μm^3 volume of stratum radiatum), a hippocampal part that correlated to the apical dendrites of CA1 pyramidal neurons, were studied with immunohistochemistry of the dendritic spine-specific protein spinophilin (Figure 3I). A significant difference among experiment groups was seen ($F_{3, 154}=4.748$, $P<0.01$). Bryostatin-1 had no effect on dendritic spine density in wild-type mice but improved the loss of dendritic spine density in the fragile X mice ($P<0.05$; Figure 3J). These data on the densities of dendritic spines per brain volume units were correlated with changes in the number of dendritic spines on dendritic spine shafts studied with DiI staining (compared Figure 3G with 3H).

Taken together, the results suggest that bryostatin-1 improves the maturation of dendritic spines from the immature spines in the young fragile X mice.

Bryostatin-1 prevents deficits in spatial learning and memory of young fragile X mice but did not alter sensorimotor ability

There were significant learning differences among the 4 groups ($F_{3,560}=58.528$, $P<0.001$; Figure 4A), indicating different learning among the groups. Spatial learning of the fragile X mice was significantly impaired (fragile X mice with vehicle vs wild-type with vehicle: $F_{1,272}=22.117$, $P<0.001$). Bryostatin-1 treatment significantly improved the learning performance of the fragile X mice (fragile X mice with vehicle vs fragile X mice with bryostatin-1: $F_{1,272}=110.621$, $P<0.001$), to the level of the control mice with bryostatin-1 treatment (wild-type with bryostatin-

JPET Fast Forward. Published on March 3, 2016 as DOI: 10.1124/jpet.115.231100
This article has not been copyedited and formatted. The final version may differ from this version.

1 vs fragile X mice with bryostatin-1: $F_{1,272}$=0.669, P>0.05), indicating that the chronic bryostatin-1 treatment not only improved spatial learning in the wild-type mice but also repaired the learning deficits of the fragile X mice when tested at an adult age after an early 6-week treatment.

The results in the probe test (Figure 4B-E) were analyzed using target quadrant ratio (dividing the target quadrant distance by the average of the non-target quadrant values during the probe test; Figure 4F). There were significant differences in the target quadrant ratio among the groups ($F_{3,38}$=8.790, P<0.001), indicating differences in the spatial memory among the groups. Detailed analysis reveals that the memory recall of the transgenic mice was impaired (fragile X mice with vehicle vs wild-type with vehicle: $F_{1,\ 18}$=5.155, P<0.05) and that bryostatin-1 treatment in the transgenic mice significantly improved the memory recall as compared with that of the fragile X mice without the treatment ($F_{1,17}$=21.145, P<0.001), to the level of the control mice with bryostatin-1 (control mice with bryostatin-1vs the fragile X mice with bryostatin-1: $F_{1,17}$=0.063, P>0.05).

A visible platform test, determined after the probe test reveals no significant differences among the groups ($F_{3,35}$=0.179 P>0.05; Figure 4G), indicating that there were no significant group differences in sensorimotor ability and escape motivation of the mice among different groups, so that the differences in the learning and memory-recall performance among the groups cannot be attributed to the differences in their sensorimotor ability and escape motivation.

JPET Fast Forward. Published on March 3, 2016 as DOI: 10.1124/jpet.115.231100
This article has not been copyedited and formatted. The final version may differ from this version.

Discussion

The main finding of the present study, an early-onset treatment in young adult mice, can be summarized as: (1) The loss of FMR1 protein in the fragile X mice suppresses BDNF expression, dendritic spine and synaptic maturation, PSD-95 and mGluR5 accumulation, and memory-dependent mushroom-shape dendritic spine formation in the apical dendrites of the hippocampal CA1 neurons, resulting in spatial learning and memory deficits. (2) The synaptic immaturity and cognitive dysfunction, core features of FXS, and other FXS phenotypes can be rescued with an early treatment of bryotatin-1, to produce therapeutic effects that are better than those of a late-onset treatment (see below). (3) The therapeutic impacts can be achieved without down-regulation of mGluR5 in the hippocampus.

It has been well established that FMRP mediates activity-dependent control of synaptic structure and function (Huber et al., 2002). Experimental studies suggest that its lack leads to in an overactivity of the mGluR5, a decreased GABAergic system (Olmos-Serrano et al., 2010), and an elevated activity of GSK3β (Guo et al., 2012). Synaptic immaturity and cognitive dysfunction are core symptoms in FXS and learned-induced formation of dendritic spines is severely impaired in the fragile X mice (Padmashri et al., 2013). Fragile X mice show an abundance of dense, immature dendritic spines (Scott-Lomassese et al., 2011), as in FXS patients (Grossman et al., 2006). The hyper-abundance of immature-looking lengthened dendritic spine could be the results of a failed/delayed maturation (Cruz-Martin et al., 2010) and activity-dependent synaptic elimination (Pfeiffer *et al*., 2010). It has been reported that the left hippocampus in young male adult fragile X permutation carriers exhibits reduced structural connectome (Leow et al., 2014), consistent with the evidence of a range of cognitive impairment, including spatial processing (Hocking et al., 2012; Wong et al., 2012). The deficit may also

involve a loss of some dendritic channels (Routh et al., 2013), but can be rescued with chronic bryostatin-1 treatment at a young age, as shown in the present study, and previously in adults (Sun et al., 2014). The treatment in the present study began at least 1 month earlier than our previous study (Sun et al., 2014), in which the same dose was administered at an adult age (2 months of age) for a longer treatment period (13 weeks). Histological analyses were all performed at an adult age. Earlier treatment may lead to more favorable outcomes due to several reasons. First, the therapeutic outcomes appear significantly better in the early-onset treatment group with the same doses of treatment, including the higher enhancement of BDNF expression and mushroom-shaped dendritic spine formation (Figure 5A,B), better synaptic maturation (Figure 5C,D), and resulted in a larger improvements in performance in the water maze task (Figure 5E,F), suggesting that the brain network under the treatment has regained the capacity to meet cognitive demands. Second, an early intervention might facilitate a more 'normal' development of socio-cognitive skills and behaviors.

Our results of reduced mGluR5 labeling in the hippocampus of fragile X mice and increased labeling with bryostatin-1 treatment are somewhat unexpected. The data suggest that syndromic features of FXS might not be caused by an upregulated mGluR5 signaling pathway and synaptic and cognitive function can be rescued without down-regulation of mGluR5 signaling. Desensitization of the mGluR5, if induced (Gereau and Heinemann, 1998), and increased internalization would result in a decreased surface expression of the receptor (Ko et al., 2012), a response not observed in the study. There is no evidence suggesting a direct association of FMRP with *Grm5* mRNA, although Lohith and co-workers revealed that both mGluR5 binding and protein expression were increased in the prefrontal cortex of FXS patients and carriers (Lohith et al., 2013). In the fragile X mouse hippocampus, Western blot analysis was reported to

find no difference in mGluR5 protein expression (Dolen et al., 2007), while a reduction was observed in the detergent insoluble fraction of synaptic membranes isolated from the forebrain of fragile X mice (Giuffrida et al., 2005). There are also some observations of reduced expression of mGluR5 in fragile X mice (Giuffrida et al., 2005), but no difference in mGluR5 expression in total hippocampal homogenates has been reported by others (Huber et al., 2002). The no differences in mGluR5 expression (Huber et al., 2002; Giuffrida et al., 2005) between fragile X mice and control but reduced association of mGluR5 with PSD in fragile X mice might suggest an increased non-PSD association of mGluR5 labeling in fragile X mice. However, the evidence that supports the notion that mGluR5 overactivity reflects neuronal pathology in FXS seems very solid. Reducing mGluR5 expression or mGluR5 inhibitors have been shown to correct a broad range of fragile X phenotypes in fragile X mice (Huber et al., 2002; Hajós, 2014). Although one would expect an increased colocalization of postsynaptic mGluR5 when it is overactive, our study does not rule out the possibility that the observed reduction in mGluR5 labeling in the fragile X mice might partially reflect the reduced PSD labeling in the brain area. Nevertheless, our results indicate that the desired therapeutic effects can be achieved in the fragile X mice without down-regulation of mGluR5 in the hippocampus. The effective treatment actually improves mGluR5 labeling in the hippocampus. It is probably appropriate to mention here that whilst preclinical studies with mGluR5 antagonism appear promising, therapeutic values of mGluR5 inhibitors for FXS are still not clear. The mGluR5 inhibition exaggerates spine immaturity in fragile X mice (Cruz-Martin et al., 2010), an effect that would be considered opposite to the intended therapeutic outcomes. In addition, basimglurant and mavoglurant, two different and potent mGluR5 inhibitors, did not show therapeutic benefit in recent phase 2 clinical trials in FXS patients (Scharf et al., 2015).

Consistent with our previous study in the fragile X mice, chronic bryostatin-1 rescues other FXS phenotypes, such as PSD-95 (Zalfa et al., 2007; Tang and Alger, 2015) and BDNF levels in the hippocampus. PSD-95, a major synapse organizer, plays an important role in the stabilization of spines and synapses and in activity-regulated formation of PSD. BDNF is important for local protein synthesis and synaptic plasticity (Neumann et al., 2015). Although images of the BDNF fluorescence labeling were used to measure the BDNF levels in this study, the labeling intensity was found to reliably reflect the BDNF levels in the same brain areas determined with an immunochemical assay, such as an ELISA assay, in our previous studies (Sun et al., 2004). Reduction of BDNF expression in fragile X mice induces cognitive deficits (Louhivuori et al., 2011; Uutela et al., 2012). Infusion of BDNF has been found to restore synaptic function in slices from fragile X mice (Lauterborn et al., 2007). The decrease in BDNF accumulation in the CA1 stratum radiatum was significantly prevented with both the early-onset (the present study) and late-onset (Sun *et al*., 2014) bryostatin-1 treatment. However, early-onset bryostatin-1 treatment, but not late-onset bryostatin-1 treatment, also enhanced the BDNF level (higher than the control wild-type without bryostatin-1 treatment).

It is interesting that in the wild-type mice, the early-onset bryostatin-1 treatment significantly elevated the spatial memory retention (in the present study) above wild-type levels, whereas the late-onset bryostatin-1 treatment did not enhance memory retention (Sun et al., 2014), with the same lag period to separate acute impact from the chronic therapeutic effects. However, we did not find a significant enhancement of PKCε-induced BDNF levels after early-onset bryostatin-1 treatment. This might implicate that other PKCε-dependent pathways might also be involved in synaptic plasticity. The direct interaction of PKCε with actin is important for synaptic function and neurite growth and synaptic formation (Prekeris et al., 1996). PKCε may also induce

JPET Fast Forward. Published on March 3, 2016 as DOI: 10.1124/jpet.115.231100
This article has not been copyedited and formatted. The final version may differ from this version.

synaptogenesis directly by activating structural changes through its phosphorylation substrates, GAP-43, MARCKS, and adducin (Matsuoka et al., 1998).

Bryostatin-1, a highly potent and relatively specific PKCε activator, with pharmacological profiles of synaptogenesis and synaptic maturation/repairing (Hongpaisan and Alkon, 2007, 2011; Sun et al., 2015), rescues synaptic and memory functions and other phenotypic features in young fragile X mice. At low concentrations (about 1 nm), its PKC activation is mostly on PKCε, and less on PKCα. At higher concentrations, however, activities of other PKC isoforms might also be affected. At a lower dose (10 $\mu g/m^2$, 2 doses/week for 3 weeks), bryostatin-1 alone was found to have no significant effects on spatial learning and memory in rats (Sun and Alkon, 2008). We previously observed that its chronic administration did not alter swimming speed of rodents in the swimming test (Sun and Alkon, 2008). Evidence is accumulating, supporting an essential role of some PKC isoforms in various phases and types of learning and memory (Alkon et al., 2005, 2007). Bryostatin-1-like agents enhance the synthesis of proteins required for memory processing and synaptic repair/synaptogenesis, reduce Aβ formation through activation of α-secretase and increase Aβ degradation via the endothelin-converting enzyme, and are anti-apoptotic. Since intellectual ability, as well as retardation (Wang et al., 2012), involves multiple players in signal processing, these agents, for their multi-targeting actions (Sun et al., 2015), may represent a more effective class of therapeutics than agents that target a single factor in this complex pathologic process (Vislay et al., 2013).

Authorship Contributions

Conducted experiments: Sun, M.-K., and Hongpaisan, J.

Performed data analysis: Sun, M.-K., and Hongpaisan, J.

Wrote or contributed to the writing of the manuscript: Sun, M.-K., Hongpaisan, J., and Alkon, D.L.

Financial Disclosures: The authors declaim no conflict interest.

References

Alkon DL, Epstein H, Kuzirian A, Bennett MC, and Nelson TJ (2005) Protein synthesis required for long-term memory is induced by PKC activation on days before associative learning. *Proc Nat Acad Sci USA* **102:** 16432-16437.

Alkon DL, Sun M-K, and Nelson TJ (2007) PKC signaling deficits: a mechanistic hypothesis for the origins of Alzheimer's disease. *Trends Pharmacol Sci* **28:** 51-60.

Ashley CT, Wilkinson KD, Reines D, and Warren ST (1993) FMR1 protein: conserved RNP family domains and selective RNA binding. *Science* **262:** 563-266.

Bhattacharya A and Klann E (2012) Fragile X syndrome therapeutics s(c)tep through the developmental window. *Neuron* **74:** 1-3.

Chen E, Sharma MR, Shi X, Agrawal RK, and Joseph S (2014) Fragile X mental retardation protein regulates translation by binding directly to the ribosome. *Mol Cell* **54:** 407-417.

Cruz-Martin A, Crespo M, and Portera-Cailliau C (2010) Delayed stabilization of dendritic spines in fragile X mice. *J Neurosci* **30:** 7793-7803.

Darnell JC and Klann E (2013) The translation of translational control by FMRP: therapeutic targets for FXS. *Nat Neurosci* **16:** 1530-1536.

Dolen G, Osterwell E, Rao BS, Smith GB, Auerbach BD, Chattarji S, and Bear MF (2007) Correction of fragile X syndrome in mice,. *Neuron* **56:** 955-962.

Glantz A, Gilmore JH, Hamer RM, Lieberman JA, and Jarskog LF (2007) Synaptophysin and PSD-95 in the human prefrontal cortex from mid-gestation into early adulthood. *Neuroscience* **149:** 582-591.

Gereau RW 4th and Heinemann SF (1998) Role of protein kinase C phosphorylation in rapid desensitization of metabolic glutamate receptor 5. *Neuron* **20:** 143-151.

Giuffrida R, Musumeci S, D'Antoni S, Bonaccorso CM, Giuffrida-Stella AM, Oostra BA, and Catania MV (2005) A reduced number of metabotropic glutamate subtype of 5 receptors are associated with constitutive homer proteins in a mouse model of fragile X syndrome. *J Neurosci* **25:** 8908-8916.

Grossman AW, Aldridge GM, Weiler IJ, and Greenough WT. (2006) Local protein synthesis and spine morphogenesis: fragile X syndrome and beyond. *J Neurosci* **26:** 151-155.

Guo W, Murthy AC, Zhang L, Johnson EB, Schaller EG, Allan AM, and Zhao X (2012) Inhibition of GSK3β improves hippocampus-dependent learning and rescues neurogenesis in a mouse model of fragile X syndrome. *Human Mol Genet* **21:** 681-691.

Hajós M (2014) Portraying inhibition of metabotropic glutamate receptor 5 in fragile X mice. *Biol Psychiatry* **75:** 177-178.

Hocking DR, Kogan CS, and Cornish KM (2012) Selective spatial processing deficits in an at-risk subgroup of the frasgile X permutation. *Brain Cogn* **79:** 39-44.

Hongpaisan J and Alkon DL (2007) A structural basis for enhancement of long-term associative memory in single dendritic spines regulated by PKC. *Proc Natl Acad Sci USA* **104:** 19571-19576.

Hongpaisan J, Sun M-K, and Alkon DL (2011) PKC ε activation prevents synaptic loss, Aβ elevation, and cognitive deficits in Alzheimer's disease transgenic mice. *J Neurosci* **31:** 630-643.

Hongpaisan J, Xu C, Sen A, Nelson TJ, Alkon DL (2013) PKC activation during training restores mushroom spine synapses and memory in the aged rat. *Neurobiol Disease* **55:** 44-62.

Horling K, Schlegel G, Schulz S, Vierk R, Ullrich K, Santer R, and Rune GM (2015) Hippocampal synaptic connectivity in phenylketonuria. *Hum Mol Genet* **24:** 1007-1018.

Huber KM, Gallagher SM, Warren ST, and Bear MF (2002) Altered synaptic plasticity in a mouse model of fragile X mental retardation. *Proc Natl Acad Sci USA* **28:** 7746–7750.

Huttenlocher PR and Dabholkar (1997) Regional differences in synaptogenesis in human cerebral cortex. *J Comparat Neurol* **387:** 167-178.

Kirov, SA, Petrak LJ, Fiala JC, and Harris KM (2004) Dendritic spines disappear with chilling but proliferate excessively upon rewarming of mature hippocampus. *Neuroscience* **127:** 69-80.

Ko SJ, Isozaki K, Kim I, Lee JH, Cho HJ, Sohn SY, Oh SR, Park S, Kim DG, Kim CH, and Roche KW (2012) PKC phosphorylation regulates mGluR5 trafficking by ejnhancing binding of Siah-1A. *J Neurosci* **32:** 16391-16401.

Koekkoek SK, Yamaguchi K, Milojkovic BA, Dortland BR, Ruigrok TJ, Maex R, De Graaf W, Smit AE, VanderWerf F, Bakker CE, Willemsen R, Ikeda T, Kakizawa S, Onodera K, Nelson DL, Mientjes E, Joosten M, De Schutter E, Oostra BA, Ito M, and De Zeeuw CI (2005) Deletion of FMR1 in Purkinje cells enhances parallel fiber LTD. Enlarges spines, and attenuates cerebellar eyelid conditioning in Fragile X Symdrome. *Neuron* **47:** 339-352.

Lauterborn JC, Rex CS, Kramár E, Chen LY, Pandyarajan V, Lynch G, and Gall CM (2007) Brain-derived neurotrophic factor rescues synaptic plasticity in a mouse model of fragile X syndrome. *J Neurosci* **27:** 10685-10694.

Leow A, Harvey D, Goodrich-Hunsaker NJ, Gadelkarim J, Kumar A, Zhan L, Rivera SM, and Simon TJ (2014) Altered structural brain connectome in young adult fragile X permutation carriers. *Human Brain Mapping* **35:** 4518-4530.

Lohith TG, Osterweil EK, Fujita M, Jenko KJ, Bear MF, and Innis RB (2013) Is metabotropic glutamate receptor 5 upregulated in prefrontal cortex in fragile X syndrome? *Mol Autism* **4:** 15.

Louhivuori V, Vicario A, Uutela M, Rantamaki T, Louhivuori LM, Castrén E, Tongiorgi E, Akerman KE, and Castrén ML (2011) BDNF and TrkB in neuronal differentiation of Fmr1-knockout mouse. *Neurobiol Dis* **41:** 469-480.

Matsuoka Y, Li X, and Bennett V (1998) Adducin is an in vivo substrate for protein kinase C: phosphorylation in the MARCKS-related domain inhibits activity in promoting spectrin-actin complexes and occurs in many cells, including dendritic spines of neurons. *J Cell Biol* **142:** 485-497.

Michalon A, Sidorov M, Ballard TM, Ozmen L, Spooren W, Wettstein JG, Jaeschke G, Bear MF, and Lindermann L (2012) Chronic pharmacological mGlu5 inhibition corrects Fragile X in adult mice. *Neuron* **74:** 49-56.

Nelson TJ and Alkon DL (2015) Molecular regulation of synaptogenesis during associative learning and memory. *Brain Res* **1621:** 239-251.

Neumann JT, Thompson JW, Raval AP, Cohan CH, Koronowski KB, and Perez-Pinzon MA (2015) Increased BDNF protein expression after ischemic or PKC epsilon preconditioning promotes electrophysiologic changes that lead to neuroprotection. *J Cereb Blood Flow Metab* **35:** 121-130.

Olmos-Serrano JL, Paluszkiewicz SM, Martin BS, Kaufmann WE, Corbin JG, and Huntsman MM (2010) Defective GABAergic neurotransmission and pharmacological rescue of neuronal hyperexcitability in the amygdala in a mouse model of fragile X syndrome. *J Neurosci* **30:** 9929-9938.

Padmashri E, Reiner B, Suresh A, Spartz E, and Dunaevsky A (2013) Altered structural and functional synaptic plasticity with motor skill learning in a mouse model of fragile X syndrome. *J Neurosci* **33:** 19715-19723.

Pfeiffer BE, Zang T, Wilkerson JR, Taniguchi M, Maksimova MA, Smith LN, Cowan CW, and Huber KM (2010) Fragile X mental retardation protein is required for synapse elimination by the activity-dependent transcription factor MFF2. *Neuron* **66:** 191-197.

Prekeris R, Mayhew MW, Cooper JB, and Terrian DM. (1996) Identification and localization of an actin-binding motif that is unique to the epsilon isoform of protein kinase and participates in the regulation of synaptic function. *J Cell Biol* **132:** 77-90.

Rodriguez A, Ehlenberger DB, Dickstein DL, Hof PR, and Wearne SL (2008) Automated Three-Dimensional Detection and Shape Classification of Dendritic Spines from Fluorescence Microscopy Images. *PLoS ONE* **3:** e1997.

Routh BN, Johnston D, and Brager DH (2013) Loss of functional A-type potassium channels in the dendrites of CA1 pyramidal neurons from a mouse model of fragile X syndrome. *J Neurosci* **33:** 19442-19450.

Sabaratnam M, Murthy NV, Wijeratne A, Buckingham A, and Payne S (2003) Autistic-like behavior profile and psychiatric morbidity in Fragile X Syndrome: a prospective ten-year follow-up study. *Eur Child Adolesc Psychiatry* **12:** 172-177.

Santoro MR, Bray SM, and Warren ST (2012) Molecular mechanisms of Fragile X Syndrome: A twenty-year perspective. *Annu Rev Pathol Mech* **7:** 219-245.

Scharf SH, Jaeschke G, Wettstein JG, Lindemann L (2015). Metabotropic glutamate receptor 5 as drug target for fragile X syndrome. *Curr Opinion Pharmacol* **20:** 124-134.

Scott-Lomassese S, Nissant A, Mota T, Néant-Féry M, Oostra BA, Greer CA, Lledo PM, Trembleau A, and Caillé I (2011) Fragile X mental retardation protein regulates new neuron differentiation in the adult olfactory bulb. *J Neurosci* **31:** 2205-2215.

Sengupta P (2013) The laboratory rat: Relating its age with human's. *Int J Prev med* **4:** 624-630.

Siomi H, Choi M, Siomi MC, Nussbaum RL, and Dreyfuss G (1994) Essential role for KH domains in RNA binding: impaired RNA binding by a mutation in the KH domain of FMR1 that causes fragile X syndrome. *Cell* **77:** 33-39.

Sorra KE and Harris KM (2000) Overview on the structure, composition, function, development, and plasticity of hippocampal dendritic spines. *Hippocampus* **10:** 501-511.

Sun M-K and Alkon DL (2008) Synergistic effects of chronic bryostatin-1 and α-tocopherol on spatial learning and memory in rats. *Eur J Pharmacol* **584:** 328-337.

Sun M-K, Hongpaisan J, Lim CS, and Alkon DL (2014) Bryostatin-1 restores hippocampal synapses and spatial learning and memory in adult fragile X mice. *J Pharmacol Exp Ther* **349:** 393-401.

Sun M-K, Nelson TJ, and Alkon DL (2015) Towards universal therapeutics for memory disorders. *Trends in Pharmacol Sci* **36:** 384-394.

Tang AH and Alger BE (2015) Homer protein–metabotropic glutamate receptor binding regulates endocannabinoid signaling and affects hyperexcitability in a mouse model of Fragile X Syndrome. *J Neurosci* **35:** 3938-3945.

Tassone F (2014) Newborn screening for fragile X. *JAMA Neurol* **71:** 355-359.

Uutela M, Lindholm J, Louhivuori V, Wei H, Louhivuori LM, Petrovaara A, Akerman K, Castrén E, and Castrén ML (2012) Reduction of BDNF expression in Fmr1 knockout mice

worsens cognitive deficits but improves hyperactivity and sensorimotor deficits. *Genes Brain Behav* **11:** 513-523.

Verkerk AJ, Pieretti M, Sutcliffe JS, Fu YH, Kuhl DP, Pizzuti A, Reiner O, Richards S, Victoria MF, Zhang F, Eussen BE, van Ommen G-J B, Blonden LAJ, Riggins GJ, Chastain JL, Kunst CB, Galjaard H, Caskey CT, Nelson DL, Oostra BA, and Stephen T. Warren (1991) Identification of a gene (FMR-1) containing a CGG repeat coincident with a breakpoint cluster region exhibiting length variation in fragile X syndrome. *Cell* **65:** 905-914.

Vislay RL, Martin BS, Olmos-Serrano JL, Kratovac S, Nelson DL, Corbin JG, and Huntsman MM (2013) Homeostatic responses fail to correct defective amygdala inhibitory circuit maturation in fragile X syndrome. *J Neurosci* **33:** 7548-7558.

Wang X, Snape M, Klann E, Stone JG, Singh A, Petersen RB, Castellani RJ, Casadesus G, Smith MA, and Zhu X (2012) Activation of the extracellular signal-regulated kinase pathway contributes to the behavior deficit of fragile x-syndrome. *J Neurochem* **121:** 672-679.

Wong LM, Goodrich-Hunsaker NJ, McLennan Y, Tassone F, Harvey D, Rivera SM, and Simon TJ (2012) Young adult male carriers of the fragile X permutation exhibit genetically modulated impairments in visuospatial tasks controlled for psychomotor speed. *J Neurodev Disord* **4:** 26.

Zalfa F, Eleuteri B, Dickson KS, Mercaldo V, De Rubeis S, di Penta A Tabolacci E, Chiurazzi P, Neri G, Grant SG, and Bagni C (2007) A new function for the fragile X mental retardation protein in regulation of PSD-95 mRNA stability. *Nat Neurosci* **10:** 578-587.

JPET Fast Forward. Published on March 3, 2016 as DOI: 10.1124/jpet.115.231100
This article has not been copyedited and formatted. The final version may differ from this version.

Figure Legends

Figure 1. Bryostatin-1 raised the levels of mGluR5, and BDNF in the hippocampal CA1 stratum radiatum of young Fragile X mice (at an age of 12 weeks). Mice were treated with bryostatin-1 or drug vehicle and behaviorally trained for spatial memory. Immunohistochemistry and confocal microscopy were performed in the hippocampal CA1 stratum radiatum. (A) Confocal immunohistochemistry of postsynaptic density protein 95 (PSD) and colocalization of mGluR5 and postsynaptic density protein-95 (PSD-95). (B) the overall density of PSD of postsynaptic membranes per 45 x 45 x 0.6 μm^3 volume of the CA1 stratum radiatum. (C) Density of postsynaptic membranes containing mGluR5. (D) The level of mGluR5 within postsynaptic membranes. (E, F) The levels of BDNF. WC, wild-type with vehicle; WB, wild-type with bryostatin-1; TC, fragile X mice with vehicle; TB, fragile X mice with bryostatin-1. Data are shown as means ± S.E.M, n = 40-55 random CA1 stratum radiatum areas from 4 mice per experimental conditions. All the images are from the stratum radiatum only. *: $P < 0.05$, **: $P < 0.01$, ***: $P < 0.001$.

Figure 2. Bryostatin-1 raised the levels of vesicle concentration in presynaptic axonal boutons in the hippocampal CA1 stratum radiatum of young Fragile X mice (at an age of 12 weeks). We have concerns about potential problems of single section analysis for presynaptic vesicle concentration using EM. Therefore, we used the immunohistochemistry to measure the presynaptic vesicle membrane protein synaptophysin intensity within the presynaptic boutons. Both EM and immunohistochemistry gave the same results. (A) Immunohistochemistry of the presynaptic vesicle membrane protein synaptophysin, imaged with a confocal microscope. (B) The density of presynaptic axonal boutons (synaptophysin grain counting). (C) The concentration of presynaptic vesicles within the axonal boutons. (D) The concentrations of

JPET Fast Forward. Published on March 3, 2016 as DOI: 10.1124/jpet.115.231100
This article has not been copyedited and formatted. The final version may differ from this version.

presynaptic vesicles within the axonal boutons, based on (E) electron microscopy at higher magnification. White arrows, presynaptic vesicles; red arrow, synapses; yellow highlighted, dendritic spines. WC, wild-type with vehicle; WB, wild-type with bryostatin-1; TC, fragile X mice with vehicle; TB, fragile X mice with bryostatin-1. Data are shown as means ± S.E.M, n = 40-55 random CA1 stratum radiatum areas from 4 mice per experimental conditions. All the images are from the stratum radiatum only. *: $P < 0.05$, **: $P < 0.01$, ***: $P < 0.001$.

Figure 3. Bryostatin-1 increased synaptic density and induced memory-dependent mushroom dendritic spine formation and dendritic spine maturation in the apical dendrites of the hippocampal CA1 pyramidal neurons in young fragile X mice (at an age of 12 weeks). Mice were treated with bryostatin-1 or drug vehicle and behaviorally trained for spatial memory. (A) Electron microscopy (yellow highlighted dendritic spines with synapses) was used to determine (B) the densities of synapses (per 14 x 14 x 0.09 μm^3 of stratum radiatum). (C) Confocal immunohistochemistry of growth-associated protein 43 (GAP-43), accumulated in presynaptic membranes, and quantification (D) presynaptic membranes per 45 x 45 x 0.6 μm^3 volume of the CA1 stratum radiatum. (E) Confocal laser scanning micrograph of DiI-stained dendritic spines on dendrites shafts. M, mushroom-shaped dendritic spine; T, thin spine; S, stubby spine; F, filopodium. The numbers (per 100 μm dendritic shaft) of (F) mushroom spines, (G) immature spines or filopodia, and (H) mushroom, thin, and stubby together. (I) Immunohistochemistry and confocal microscopy of the dendritic spine-specific protein spinophilin was used to determined (J) the density of dendritic spines (per 45 x 45 x 0.6 μm^3 of stratum radiatum). WC, wild-type with vehicle; WB, wild-type with bryostatin-1; TC, fragile X mice with vehicle; TB, fragile X mice with bryostatin-1. Data are shown as means ± S.E.M, n = 21-46 random apical dendritic

JPET Fast Forward. Published on March 3, 2016 as DOI: 10.1124/jpet.115.231100
This article has not been copyedited and formatted. The final version may differ from this version.

shafts or n = 40 random CA1 stratum radiatum areas from 4 mice per experimental conditions from 4 mice per experimental conditions. All the images are from the stratum radiatum only. *: $P < 0.05$; **: $P < 0.01$; ***: $P < 0.001$.

Figure 4. Bryostatin-1 restores spatial learning and memory in young fragile X mice. **A**. Water maze learning. Data are shown as means±SEM, using the daily 2 trials as a block. **B**-**F**. Results of the probe tests after the training trials shown as the distance in each quadrant (**B**-**F**). Data are shown as means+SEM. The quadrant 4 was the target quadrant. **F** shows target quadrant ratio. **G** shows the escape latency during the visible platform test. *: $P<0.05$; NS: $P>0.05$.

Figure 5. Chronic bryostatin-1 achieves better therapeutic effects in the early-onset than the late-onset treatment in the fragile X mice. (A-E) Effects on BDNF and synapses. Data (means±SEM) are compared ratios between transgenic mice with bryostatin-1 (TB) and their matched wild-type mice. The early-onset treatment (data in the present study) not only recovered but also elevated above wild-type levels **A**: the expression of BDNF, the densities of **B**: mushroom spines, and **C**: axodendritic synapses in the fragile X mice to the level higher than the wild-type control level (dashed lines). **D**: The early-onset treatment was also more effective to reduce the number of immature dendritic filopodia. Data for the late-onset treatment were from Sun et al., 2014 (paired *t* tests). **E-F:** Chronic bryostatin-1 achieves better therapeutic effects in the early-onset than the late-onset treatment in the fragile X mice. **E**: Water maze learning. Data are compared using their matched daily trial results (the escape latency of the treated mice/that of the untreated multiplies 100; i.e., the daily escape latency of the untreated fragile X mice as 100%) and are shown as means±SEM, **F**: Memory retention. Data are compared using their target quadrant

distance in the probe test (the target quadrant distance of the treated mice/that of the untreated multiplies 100; i.e., the target quadrant distance of the untreated fragile X mice as 100%) and are shown as means+SEM. The levels of learning and memory recall of late-onset treated fragile X mice are about those of the age-matched untreated control mice (arrows). *: $P<0.05$.

JPET Fast Forward. Published on March 3, 2016 as DOI: 10.1124/jpet.115.231100
This article has not been copyedited and formatted. The final version may differ from this version.

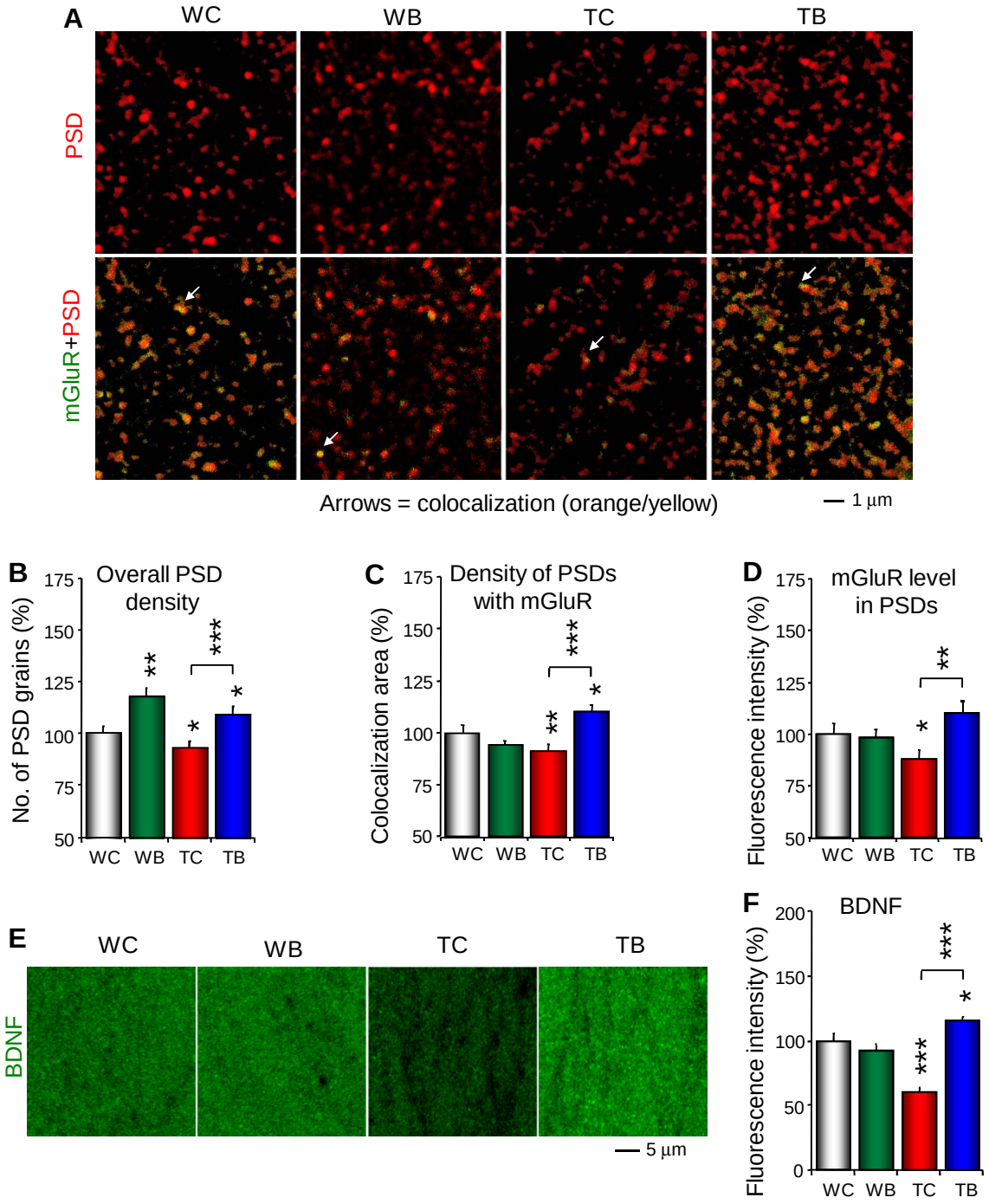

Figure 1

JPET Fast Forward. Published on March 3, 2016 as DOI: 10.1124/jpet.115.231100
This article has not been copyedited and formatted. The final version may differ from this version.

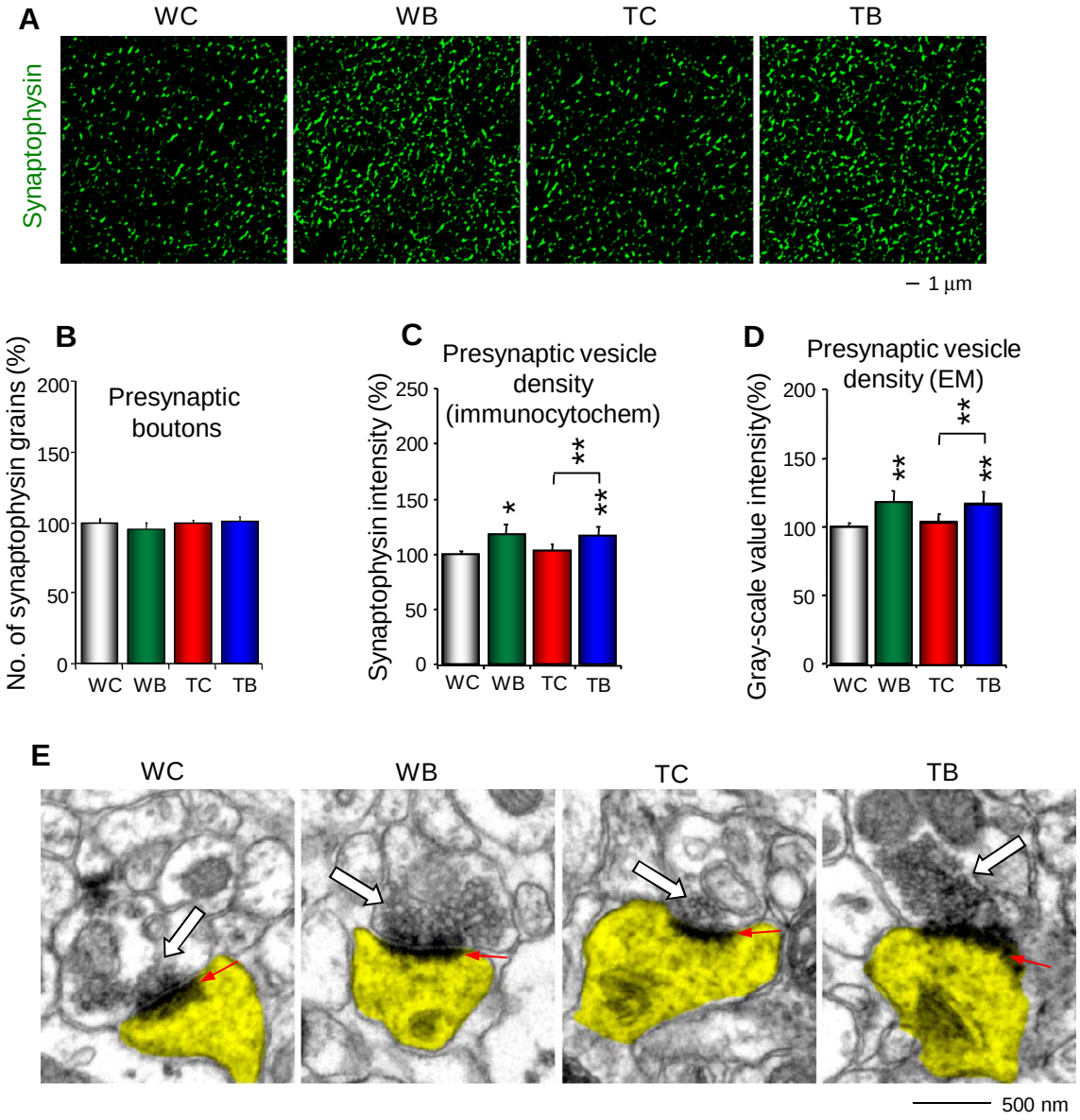

Figure 2

JPET Fast Forward. Published on March 3, 2016 as DOI: 10.1124/jpet.115.231100
This article has not been copyedited and formatted. The final version may differ from this version.

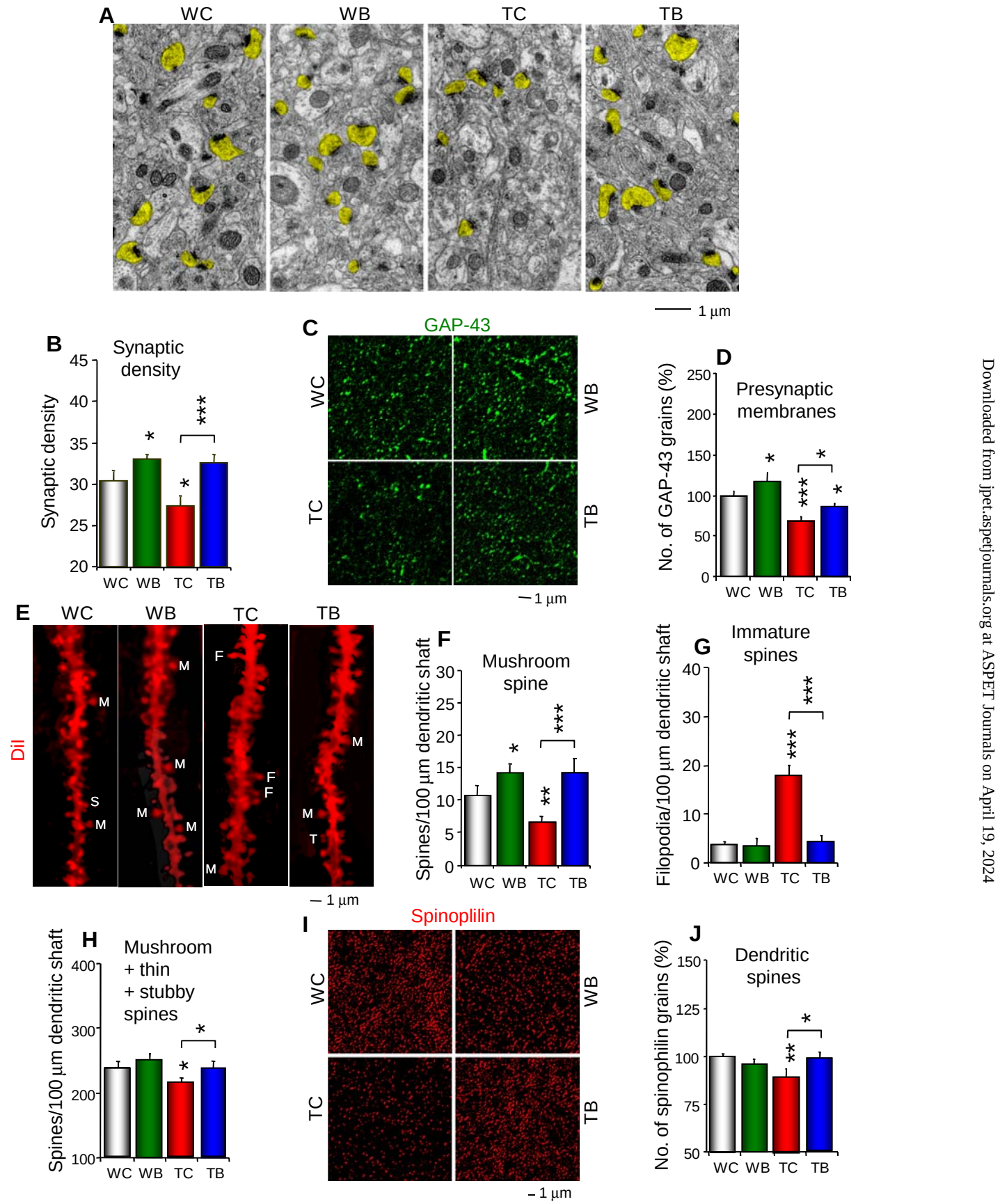

Figure 3

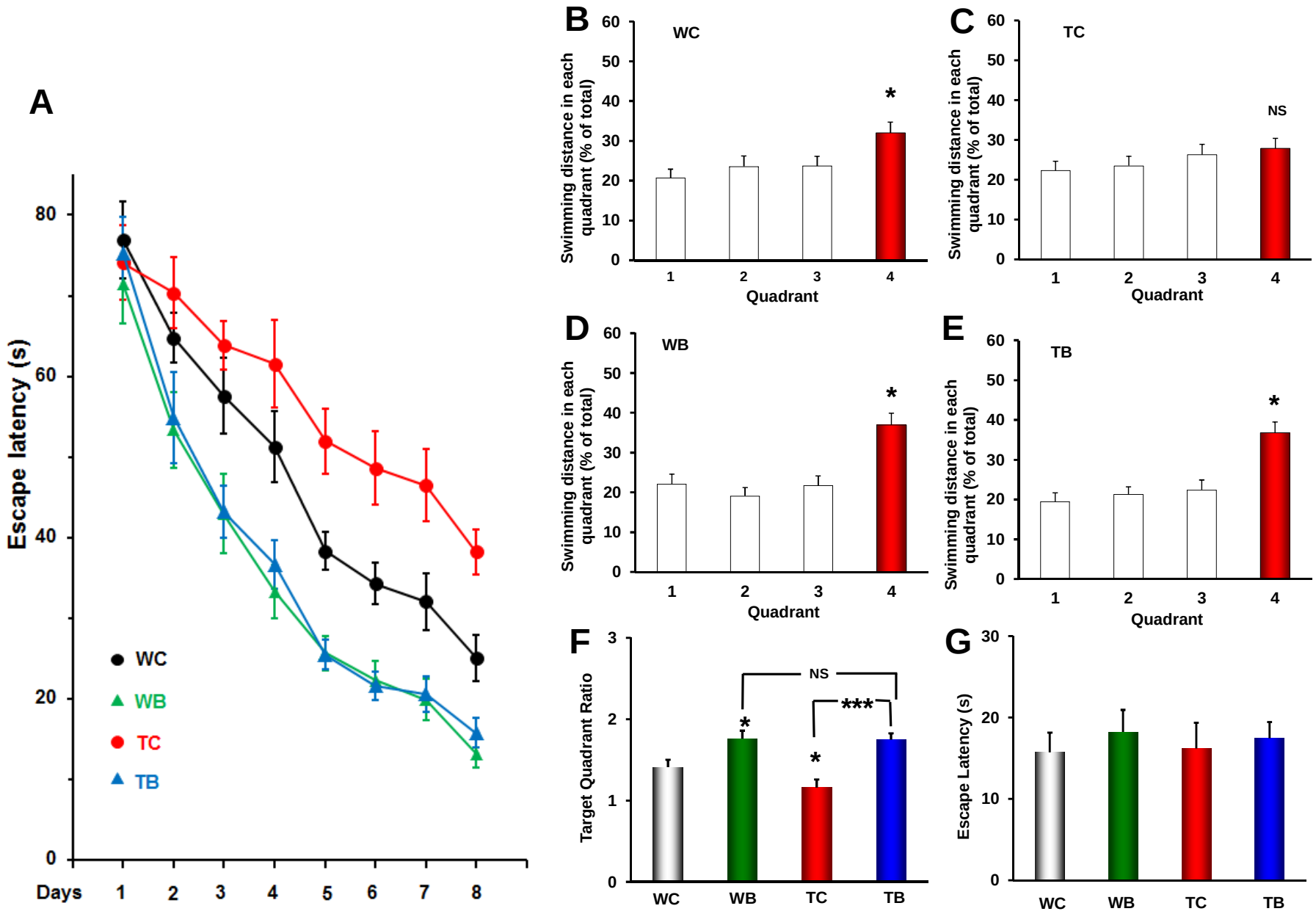

Figure 4

JPET Fast Forward. Published on March 3, 2016 as DOI: 10.1124/jpet.115.231100
This article has not been copyedited and formatted. The final version may differ from this version.

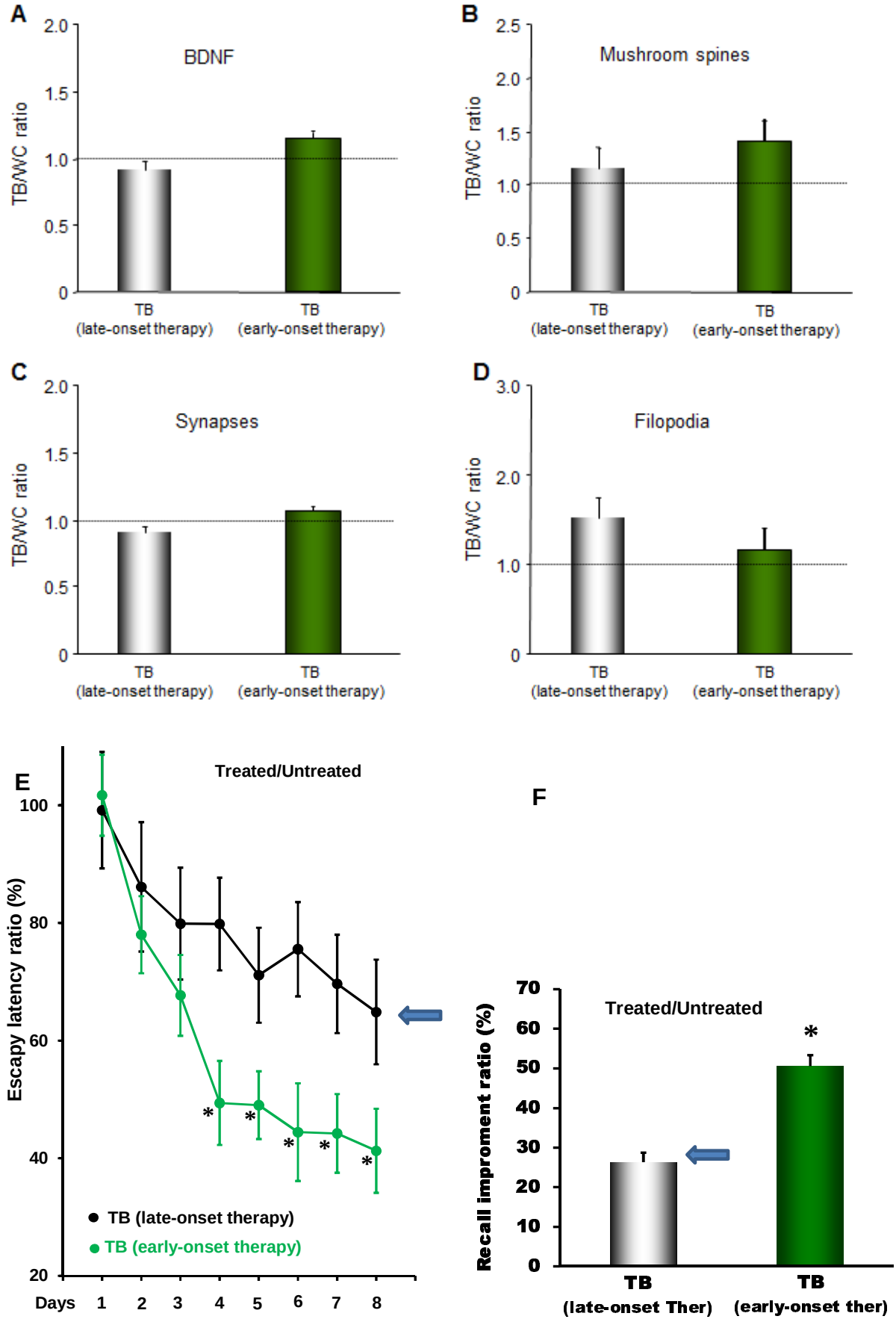

Figure 5